Bublikova T.M., Balitsky V.S., Setkova T.V., Nekrasov A.N. **Macro- and microdefects in synthetic malachite, causes of formation**

Institute of Experimental Mineralogy RAS, Chernogolovka Moscow district (tmb@iem.ac.ru)

Abstract. The synthetic malachite samples were obtained by two different methods: in an open flow system (VNIISIMS) and a closed recirculation system (IEM RAS).The typical macro- and microdefects in synthetic malachite samples were established and the causes of their formation were considered. It is shown that the defects are the main cause of the decrease in the density of malachite and are due to changes in temperature and heat-mass transfer parameters during its crystallization. The developed methods of malachite synthesis make it possible to control and prevent formation of the defects and to receive malachite, close in quality to natural malachite.

Keywords: *synthesis, malachite, ammonium solution, macro- and microdefects, density*

In the paper present results of studies of the internal structure of synthetic malachite, the basic copper carbonate [$Cu_2CO_3(OH)_2$]. Malachite was synthesized by two different methods: 1- in open flow system using ammonium copper-sulfate solutions (VNIISIMS, Aleksandrov) [Timokhina et al., 1983] and 2- in a closed recirculation system using ammonium copper-carbonate solutions (IEM RAS, Chernogolovka) [Balitsky et. al., 1987]. The methods made it possible to obtain practically all popular varieties of malachite with a various texture. The pattern of synthetic malachite is characterized by the alternation of zones from light to dark green, almost black. Morphological characteristics and physicochemical properties of synthetic malachite were studied and described in a number of publications in a comparison with natural malachite [Balitsky et al., 1987; Bublikova et al., 2000; Bublikova et al., 2017]. X-ray phase analysis and IR-spectroscopic studies of the samples were unable to reveal differences in the structure of natural and synthetic malachite. The chemical composition of synthetic and natural malachite practically has no difference in main components. However, a content of volatile components in synthetic malachite on 1.5 - 2.0 wt. % higher than in the natural malachite. The authors of the malachite synthesis method developed at St. Petersburg State University (St. Petersburg) also noted that samples of synthetic malachite at heating to 35-40 ° C, show a mass loss of 0.5-1.0 wt. % [Petrov et al., 1980; Shuyskiy, 2015]. Measurements of the density of malachite of different origin were performed by T.V. Chernenko and E.P. Melnikov [Chernenko, Melnikov, 2003] and have shown that the density of synthetic malachite on 7-16 % less than that of natural malachite. The internal structure of synthetic malachite has been studied to determine the possible causes of reduced its density. Nine samples of fine-veined texture were synthesized on vertical seeds in an open flow system; eight samples of banded and kidney-like texture were obtained in a closed system using recirculating-type crystallizers. Samples of malachite were studied with optical (MBS-10) and polarized (Nikon Eclipse LV100pol) microscopes. The phase identification was carried out on Bruker D8-advance X-ray diffractometer. The internal structure of the samples was studied on chips and polished surfaces using a Tescan Vega II XMU scanning microscope with an INCA Energy 450 energy-dispersive spectrometer (EMC) with an INCA x-sight semiconductor Si (Li) detector and an INCA Wave 700). The samples were previously coated by gold (5 nm layer thickness). The images in backscattered electrons (BSE) and secondary electrons (SE) were obtained with an accelerating voltage of 20 kV and an electron probe current of 10 nA (estimated electron beam size was 24.6 nm).

Malachite that was grown in an open flow system often has visually distinct irregularly shaped cavities up to several millimeters in size (Fig. 1*a*). The walls of the cavities are composed of malachite buds, consisting of alternating layers of small and large spherulites (Fig. 1*b*). The size of the buds does not exceed a few millimeters in diameter. The buds, as a rule, are located close to each other and often overlapped, forming a dense malachite layer. The causes of forming these cavities are following. New portions of the saturated working solution are constantly fed into the crystallizer to ensure a continuous process of malachite sedimentation. The mass nucleation of differently oriented malachite spherulites occurs on seeds, walls and bottom of the crystallizer. The newly formed buds expand, come into contact with neighboring ones and gradually block the access of the solution to the buds of the previous generation. The cavities up to 2 - 3 mm in size appear in places where there is no contact. Usually, these cavities contain remnants of the working solution. The incessant intermixing of the solution by carbon dioxide also leads to the formation of cavities and small pores. Malachite, obtained in an open system on vertical seeds, usually has a small-speckled texture, alternating with contrasting, differently colored areas. The degree of supersaturation of the solution and the set temperature fluctuations in the crystallization zone lead to color change of the growing malachite. Layers of dark green color are composed of larger aggregates of malachite than light layers that often have a cryptocrystalline structure. Only on the micro level, the pores of an irregular shape with a size of 1 - 3 μm are distinguishable in the light green zone of a dense cavities-free fine-grained malachite. In the dark green malachite layer, the pore quantity decreases but pore size increases to 20 μm. (Fig. 1*c*).

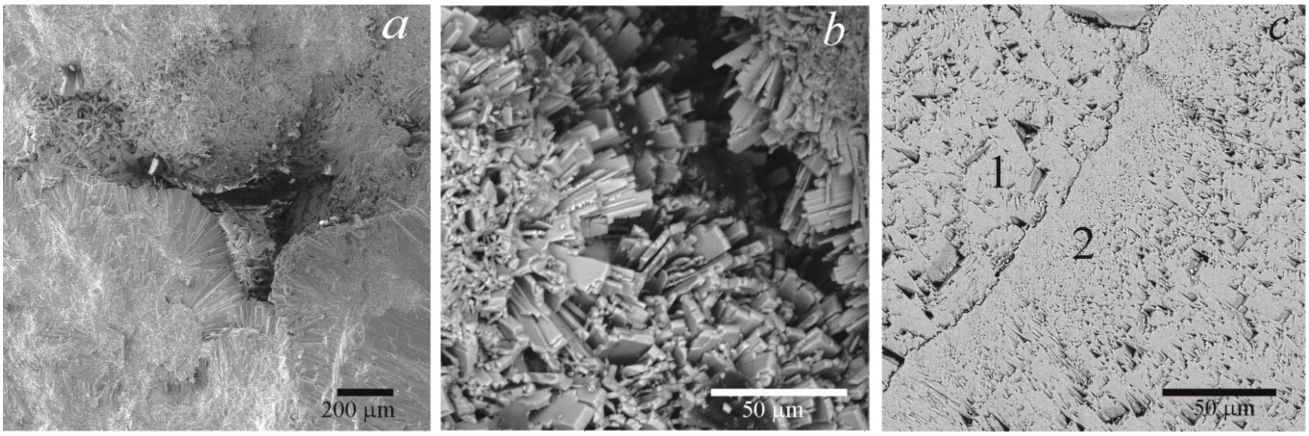

Fig. 1. SEM images of synthetic malachite samples, grown in an open flow system (VNIISIMS): *a* - micro-cavities in the cleft of the overgrown layer; *b* - formation of small pores and cavities between malachite buds; *c* - boundary of the different colored zones: 1 - dark green zone, 2 - light green zone.

The micro-cavities in malachite samples that obtained in a closed recirculation-evaporation system at the smooth change in the temperature regime of crystallization are generally not observed. A sharp increase in the temperature of the process, especially on the first day of experiment, leads to the formation of vertical tubular channels with a diameter of 1 to 3 mm in the growing layer of malachite (Fig. 2*a*). The formation of the channels is due to the fact that during the crystallization of malachite, volatile components of the solution (water, carbon dioxide, and ammonia) are constantly evaporated. The intensity of the mass transfer process increases as a temperature in the crystallizer increases. Malachite does not precipitate in the areas of continuous bubble formation of the gas mixture, that leads to the appearance of morphologically distinct hollow channels in the total mass of the growing layer of malachite. If the temperature in a crystallizer decrease, the process of mass transfer slows down until the separation of gas bubbles ceases, that leads to the filling of the channels with new malachite crystals. Similar objects, named as "gasmites" or "amphora", are described for natural and synthetic malachite [Sletov, 2015; Shuyskiy, 2015]. Of the other macro defects that reduce the density of synthetic malachite, it is necessary to note cracks arising as a result of stresses with a sharp change in the crystallization temperature. In banded malachite and in malachite buds at the micro level, the same patterns of porosity variation in the different colored layers are observed, as in fine microsphere malachite. Both in banded and in buds-like synthetic malachite, in the transition zone from the thin-crystalline (light-green color layer) malachite to the zone composed of larger aggregates (the layer of dark green color), as a rule, the pores are much larger, their size reaches 5 - 7 µm (Fig. 2*b*, 2*c*).

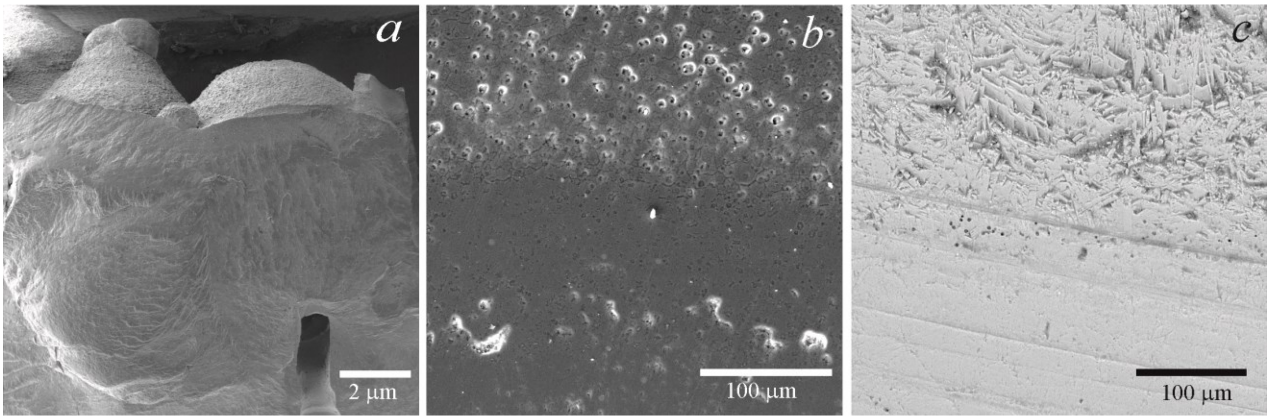

Fig. 2. SEM images of synthetic malachite samples grown in a closed recirculation system (IEM RAS): a - tubular channel penetrating a malachite sample; b and c - microporous layers in banded malachite; the upper part of the photo is a dark green zone, the lower part is a light green zone.

In the samples of synthetic malachite obtained by two in essence different methods, the most frequently encountered macro- and micro defects are irregularly shaped cavities, tubular hollow channels, micro cracks and pores of various shapes and sizes. These defects are the main cause of the decrease in the density of malachite and are due to a change in the crystallization temperature and heat and mass transfer parameters. The presence of these defects worsens the artistic and decorative qualities of malachite. The developed by us methods of malachite synthesis make it possible to control and timely prevent the formation of that defects and to receive malachite, close in quality to natural malachite.

References:

Bublikova T.M., Balitsky V.S., Timokhina I.V. Synthesis and basic properties of jewelry malachite. Synthesis of minerals. T. 1. Alexandrov, VNIISIMS. 2000. 662 p.
Petrov T.G., Moshkin S.V., Zhogoleva V.Yu. Comparative study of the morphological and physicochemical characteristics of synthetic and natural malachite. Proceeding of Leningrad Society of Naturalists. 1980. Vol. 79. V. 2. P. 142-151.
Sletov V.A. Malachite: false pseudo stalactites and "bubble gasmites" // New data on minerals. 2015. Vol. 50. P. 117 - 122.
Timokhina I.V., Balitsky V.S., Shaposhnikov A.A., Bublikova T.M., Akhmetova G.L., Dubovsky A.A Physico-chemical studies of synthetic malachite // DAN USSR. 1983. V. 270. P. 1117 - 1119.
Chernenko T.V., Melnikov E.P., Properties and diagnostics of natural and synthetic malachite // Reporter gemology. 2003. №. 8-9. P. 11-26 (№ 8). P. 31-35 (№ 9).
Shuyskiy A.V. Experimental mineralogy and genesis of synthetic malachite: dis. cand. geol.-min. sciences. St. Petersburg, St. Petersburg State University, 2015. 185 p.
Balitsky V.S., Bublikova T.M., Sorokina S.L., Balitskaya L.V., Shteinberg A.S. Man-made jewelry malachite // Gems and Gemology. 1987. V. 23. P. 152-157.
Bublikova T.M., Balitsky V.S., Setkova T.V. Features of Morphology of Synthetic Malachite // Experiment in Geosciences. 2017. V. 23. №. 1. P. 146 - 148.

Zharikov A.V.[1], Vitovtova V.M.[2], Lebedev E.B.[3], Rodkin M.V.[4]

Permeability of the continental crust: a correlation of the experimental, geological and geophysical data

UDC 551.14

[1]*Institute of Geology of Ore Deposits, Petrography, Mineralogy, and Geochemistry, Moscow,*
[2]Institute of Experimental Mineralogy, Chernogolovka,
[3]V.I. Vernadsky Institute of Geochemistry and Analytical Chemistry, Moscow,
[4]Institute of Earthquake Prediction Theory and Mathematical Geophysics, Moscow, vil@igem.ru

Abstract. A correlation between the results of the experimental study of permeability of tight rocks carried out under high temperature and pressure, geological and seismic data is presented.

Keywords: *permeability; experiment; high temperature and pressure; continental crust; seismicity*

Rock permeability governs the fluid regime, mass and heat transfer in the continental crust. At the present time there are no any remote geophysical method available for direct determination of permeability of deep seated rocks. However, permeability data at high *PT,* simulating the *in situ* conditions, can be obtained in the laboratory on relevant rock samples. This paper presents the results of permeability studies on the tight rock samples at *PT* conditions of the deep continental crust and metamorphic transformations, as well, in comparison with geological and seismic data.

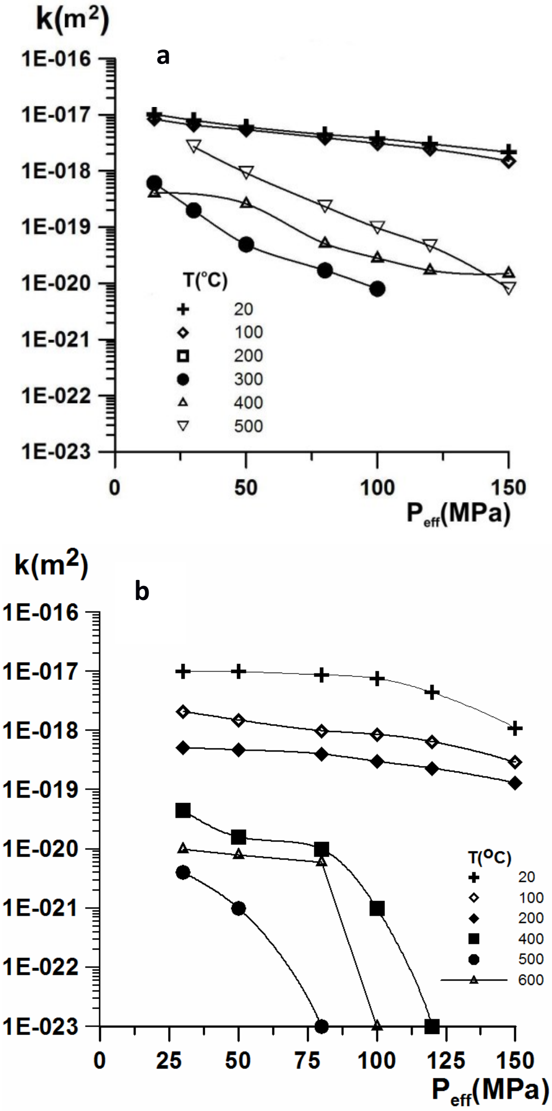

Fig. 1. Permeability vs effective pressure, T=const.a – diorite, b- amphibolite (KTB superdeep, 3847 m).

It is found that permeability is strongly and in a complicated manner controlled by competitive effect of temperature and effective pressure [Shmonov et al., 2002]. With effective pressure increase (at T=const) permeability, as a rule, decreases (Fig. 1). Temperature increase at constant effective pressure leads to monotonous permeability increase or decrease within the entire temperature range, or to appearance of inversions on the trends: permeability firstly decreases, reaches its minimum and then increases (Fig. 2). It is significant that in all cases the range of change in permeability values reaches several decimal orders of magnitude.

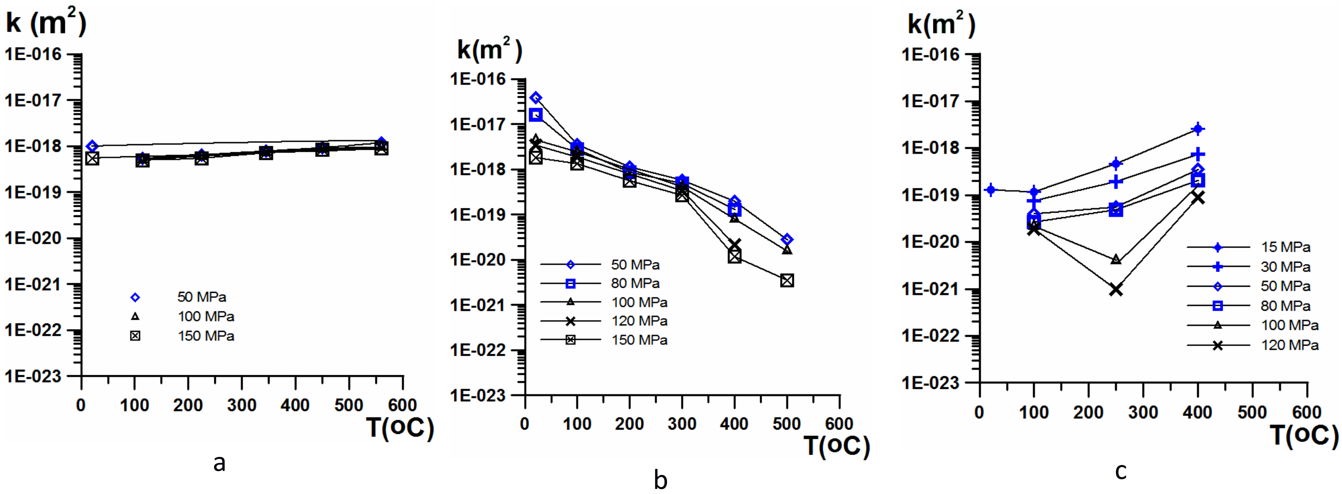

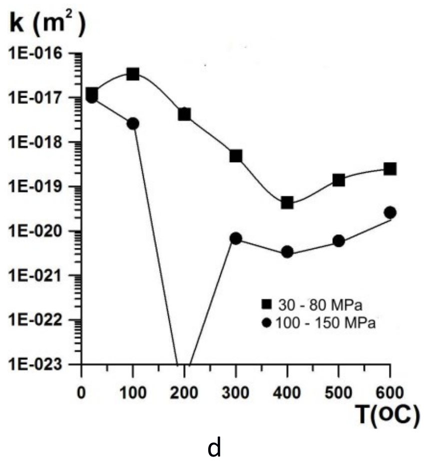

Fig. 2. Permeability vs temperature, P_{eff}=const. a – marble, b – granodiorite, c – granite, d – amphibolite (Kola superdeep, 11400 m)

On the basis of the experimental data obtained on the samples of typical rocks of the continental crust (11 samples, 234 experimental points) with simultaneous increase of temperature and pressure, simulating the *in situ* depth increase, the permeability trend with depth [Shmonov et al., 2003] was developed. The pressure effect prevails and, as a result, permeability monotonously decreases with depth. The trend is described by the relation: $\lg k = -12.6 - 3.23H^{0.223}$, where k is permeability (m^2), H is depth (km).

Such diverse permeability behavior is explained by the fact that in contrast to the other petrophysical properties, it does not depend mainly on the rock composition, but it is governed by the structure of its pore space: interconnected pores and cracks. Studies under a scanning electron microscope show that due to the effect of temperature and pressure rock microstructure can undergo strong and various transformations. For example, under heating long (low aspect ratio) microcracks, which cut many mineral grains, close, and at the same time short (high aspect ratio) ones, located at the mineral grain boundaries, on the contrary, open. [Zharikov et al., 2003]. As it is shown by SEM studies, the mineral grain microcracks are the main fluid-conducting channels at this scale level. Local processes of microcrack closure and formation can take place simultaneously and their superposition leads to occurrence of inversions on the temperature trends. Since the connectivity of fluid-conducting clusters is the governing factor responsible for permeability of tight rocks, even minor changes in microcrack density, length, aperture or interconnectivity under high PT-parameters are able to cause dramatic changes in permeability. Therefore, the sharp, threshold transitions are specific for permeability trends (Fig. 1 b, 2).

Direct *in situ* permeability measurements using hydraulic tests are usually performed at depths of no more than 3-5 km. Only a few measurements were made in superdeep wells SG-3 (Russia) and KTB (Germany) to the depth of about 10 km [Huenges et al., 1997; Kozlovsky, 1987]. So~~,~~ let us compare our estimations of the deep continental crust permeability with those obtained on the base of geological and geophysical data. In Fig. 3 curve 1 shows the trend based on our experimental data [Shmonov et al., 2003]. A large confidence interval of the dependence (indicated by a fill) shows significant variations of experimental permeability values. The permeability, calculated from the geothermal data and fluid flow flux in metamorphic systems [Ingebritsen &

Manning, 1999], also decreases with depth according to the power law (curve 2). Similar dependencies are given in [Saar & Manga 2004].

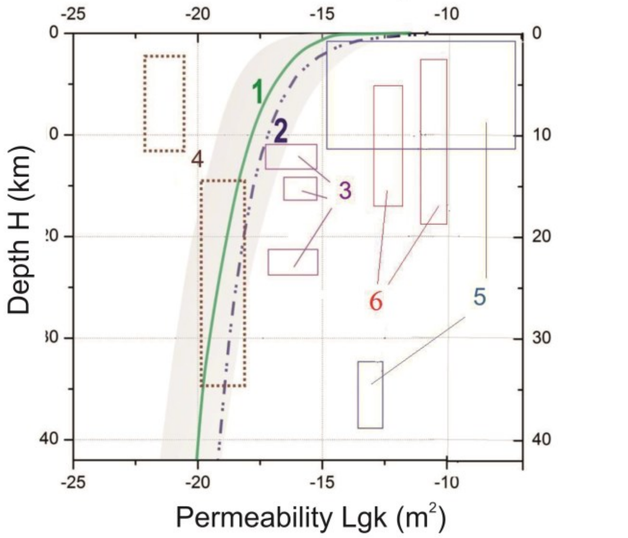

Fig. 3. Typical values of permeability in the crust according to experimental, geophysical and geological data. 1 - experimental data [Shmonov et al., 2003]; 2, 3 - estimations based on geothermal data and fluid flux during progressive metamorphism [Ingebritsen & Manning, 2010], 4 - estimations based on geophysical data [Vanyan, et, al., 2001], 5, 6 – estimations from seismological data [Ingebritsen & Manning 2010, Rodkin & Mandal, 2012].

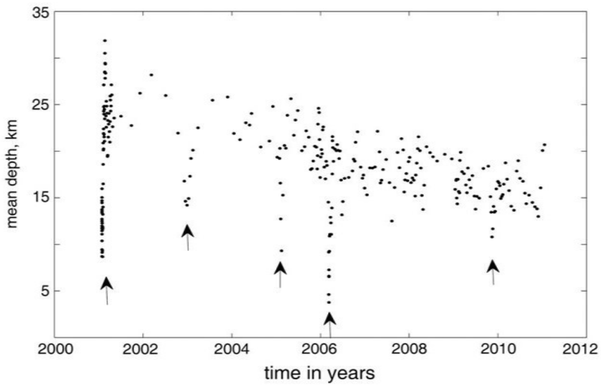

Fig. 4. Mean values of depth for groups of 20 consecutive events in the 2001 Bhuj earthquake sequence with time expired from the Bhuj mainshock occurrence.

The values of "geothermal "permeability in the entire depth range are a decimal order higher than the values of "experimental" one, which corresponds to the stable craton condition. Thus, as noted in [Ingebritsen & Manning, 2010], the trends of permeability with depth are quite consistent. Much higher permeability values may be caused by fault-zone metamorphism. Some other evidences of high permeability are obtained, revising the time scale of regional metamorphism, which is considered to be one decimal order shorter (Fig. 3, - 3) [Ingebritsen & Manning, 2010]. Permeability values calculated from magnetotelluric data are presented in [Vanyan et al, 2001]. For the depth interval of 15 – 35 km there are obtained the values close to ours and for the upper crust – the values of permeability are significantly less (Fig. 3, - 4). The highest permeability values are estimated from seismological data (Fig. 3, - 5, 6). However, the experimental study of each sample includes permeability measurements in a wide range of *PT*-parameters. From Fig. 2.4 it can be seen that under high temperature and low effective (high pore) pressure the effect of heating prevails, and, as a result, permeability increases and reaches higher values that agrees better with seismological data.

In the seismic regime the periods of extraordinary high seismic activity with unusual properties presumably associated with the fluid activity can be found. The example of the aftershock sequence of Bhuj earthquake examined in details (Mw7.7, 2001, India) is presented in Fig. 4. Besides the anomalies of b-value and mean depths, increase of apparent stresses in the seats and decrease of fractal (correlative) dimensions of their hypocenters are typical for the “bursts” of seismicity. We suppose that such bursts of seismic activity are related to ejection of the deep fluids to the Earth's surface [Rodkin & Mandal, 2012]. The effective background permeability of the mid-crust in the region of Bhuj 2001 earthquake was evaluated according to the tendency of aftershock shifting with depth and was estimated according to [Miller et al., 2004] to be about of 10^{-13} m^2.

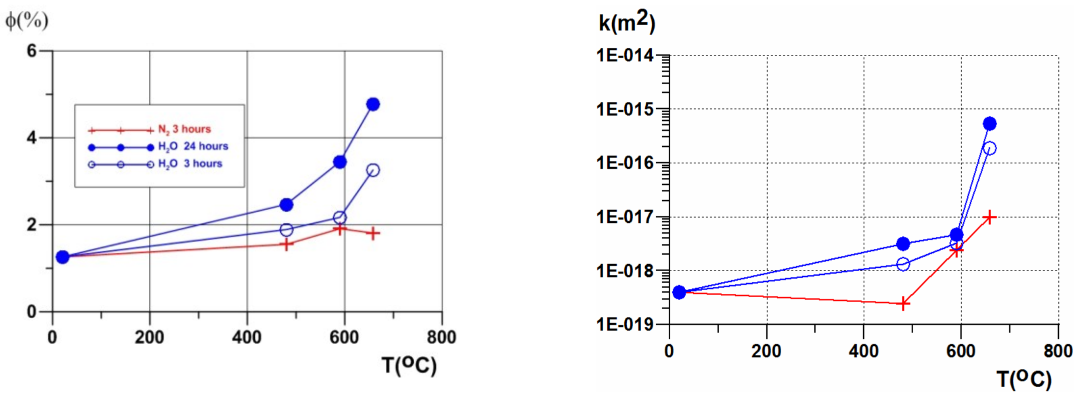

a b

Fig. 5. Dependencies of porosity (a) and permeability (b) of amphibolite heated under gas pressure in dry conditions and under water pressure P_{conf}=P_{fl}=300 MPa with different exposure time on quenching temperature.

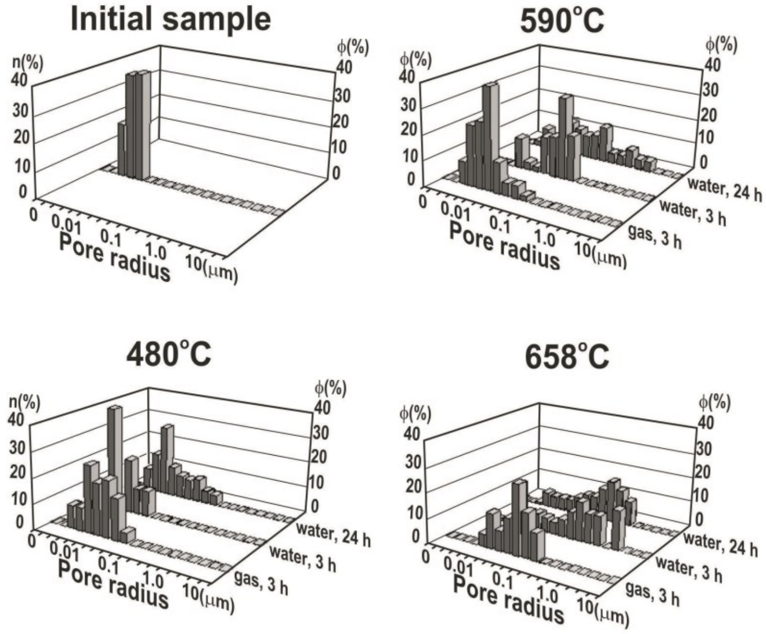

Fig. 6. Pore radius distributions for gas and water pressurized samples with different exposure time vs quenching temperature.

The experimental data presented above also show possible occurrence of high permeability horizons in the middle and low crust. The permeability increase at *PT*-parameters of progressive metamorphism: high temperature and low effective pressure (Fig. 2, 4) [Shmonov et al., 2002, Zharikov et al., 2003]. However, it should be noted, that these results are obtained in "dry" conditions in accordance with the peculiarities of the experimental procedure [Shmonov et al., 2002]. Meanwhile, the presence of water, which is the surface-active fluid, can significantly reinforce thermal decompaction of rocks. So, under these conditions a drastic increase of permeability can be caused by a positive feedback between microcrack formation in the process of the rock metamorphic transformation, leading to permeability increase and activating the fluid flow, and in turn accelerating the processes of metamorphism and microcrack initiation as it was supposed in [Ingebritsen & Manning, 2010]. We believe that the experimental data given below support this assumption. The temperature dependences of porosity and permeability for dry amphibolite samples heated in nitrogen (that does not interact with the rock matrix) or saturated by distilled water are presented in [Zharikov, 1993, 2000]. It was found that both - porosity and permeability - increase with heating. However, their values for water-saturated samples are higher than for gas-saturated ones in the entire temperature range (Fig. 5). Note, that prolongation of exposure time at higher temperature leads to further increase of porosity and permeability in the water-saturated samples due to formation of dilatational microcracks located, as a rule, along mineral grain boundaries. As a result, pore size distributions shift to the higher values. (Fig. 6).

An important issue in consideration of laboratory data is how to account a scale effect. Correlating permeability data obtained on the samples and in the shallow borehole tests Brace (1980) had found that permeability of rock massif is usually three decimal orders higher than that as measured on the samples due to fracture occurrence. However, it is not clear is this trend true under conditions of great depths. The convincing data on fracture occurrence at great depth are not still available. According to the results of the tests carried out in the Russian superdeep borehole SG-3 at depth of about 6.5 km [Kozlovsky, 1987] permeability value is very low what agree with laboratory data at appropriate PT [Zharikov et al., 2003] . In contrast in the German superdeep KTB the deep fracture zone was found [Huenges et al., 1997]. Correlating data on SG-3 and KTB, one can see that they have something in common. A presence of fluids was revealed in the both boreholes at the depth previously considerable as unreachable for them (up to 9 km in KTB and up to 11 km in SG-3). At the same time in KTB a hydraulic communication between the deep fracture zone at the depth of about 9.1 km with shallow one was found [Huenges et al., 1997]. Of course, these factors are even more unclear for the deep crust, but consideration of mentioned above data permits to suppose that, in contrast with the near-surface parts, where the fractures are uniformly distributed, in deep crust such aquifers can occur only locally. Therefore, we can assume that the decimal orders of difference between permeability values obtained with the use of experimental and seismological data show that in addition to microcracks large scale discontinuities - fractures -

appear and their formation, obviously, is expressed in aftershock bursts that were presented above (Fig. 4).

Conclusions

The experimental results show that the values of rock permeability can change by decimal orders due to the competitive effect of high temperature and pressure. It was found that, in general, permeability of the continental crust rocks decreases with depth [Shmonov et al., 2002]. In contrast, it increases at *PT*-parameters of progressive metamorphic transformations [Shmonov et al., 2002; Zharikov et al., 1993].

The results of geological studies reveal the marks of high permeability during the metamorphic processes.

The occurrence of high permeability in the deep crust is supported by seismic data. The burst of aftershocks clouds to the Earth surface and their systematical movement up to the Earth surface are found using the seismological data. Identification of such events with front of fluid pressure propagation allows to estimate high permeability values as $\approx 10^{-13}$ m^2 according to [Miller et al., 2004].

However, the mechanism of increase of permeability of mid-crust is unclear. Moreover, we suggest that some episodes of the crust permeability increase could be related to the positive feedbacks between microcrack initiation due to rock metamorphic transformations, resulting in increase of permeability and active deep fluid infiltration, which in its turn accelerates the rate of metamorphic transformations. The experimental data [Zharikov et al., 1993, 2000] prove this suggestion.

References:

Brace W.F. Permeability of crystalline and argillaceous rocks // International Journal of Rock Mechanics & Mining Sciences & Geomechanics Abstracts. - 1980. - V.17, № 5. - P. 241-251.

Ingebritsen S. E., Manning C.E. Permeability of the continental crust: dynamic variations inferred from seismicity and metamorphism // Geofluids. - 2010. - V. 10. - P. 193–205.

Kozlovsky, Ye. A. (Editor). The Superdeep Well of the Kola Peninsula. – Berlin.: Springer, 1987. -558 p.

Miller S.A., C. Collettini, L. Chiaraluce et al. Aftershocks driven by a high pressure CO_2 source at depth. // Nature. - 2004. - V. 427. - P. 724-727.

Saar M.O., Manga M. Depth dependence of permeability in the Oregon Cascades inferred from hydrogeologic, thermal, seismic, and magmatic modeling constrains. // Journal of Geophysical Research. - 2004. - V. 109. - № B4. doi:10.1029/2003JB002855

Shmonov V.M., V.M. Vitovtova, A.V. Zharikov. Fluid permeability of the rocks from the Earth crust. - Moscow: Nauchniy Mir. – 2002. 216 p. (in Russian)

Shmonov V.M., Vitovtova V.M., Zharikov A.V., Grafchikov A.A. Fluid Permeability of the Continental Crust: Estimation from Experimental Data. // Journal of Geochemical Exploration. - 2003. - V. 78-79. - P. 697-699.

Rodkin M.V., Mandal P. A possible physical mechanism for the unusually long sequence of seismic activity following the 2001 Bhuj Mw7.7 earthquake, Gujarat, India. // Tectonophysics. - 2012. - V. 536–537. P. 101-109.

Vanyan, LL, Berdichevski, MN; Kuznetsov, VA; Palshin, NA; Kong, XR; Yan, Y; Zhao, G Electromagnetic constraints on the East Tien Shan crust: Analysis of the TM mode. // Izvestiya-Physics of the Solid Earth. - 2001. - V. 37, № 3. - P. 234-243.

Zharikov A.V., Lebedev E.B., Dorfman A.M., Vitovtova V.M. Effect of saturating fluid composition on the rock microstructure, porosity, permeability and Vp under high pressure and temperature. // Physics and Chemistry of the Earth. - 2000. – V. 25, № 2. – P. 215-218.

Zharikov A.V., Pek A.A., Lebedev E.B., Dorfman A.M., Zebrin S.R. The effect of water fluid at temperature up to 850 ^{o}C and pressure of 300 MPa on porosity and permeability of amphibolite. // Physics of the Earth and Planetary Interiors. - 1993.- V 76, № 3/4. - P 219-227.

Zharikov A.V., Vitovtova V.M., Shmonov V.M., Grafchikov A.A. Permeability of the rocks from the Kola superdeep borehole at high temperature and pressure: implication to fluid dynamics in the continental crust. // Tectonophysics. - 2003. - V. 370, № 1-4. - P. 177-191.